

Synthesis and MAO inhibitory activity of novel thiazole-hydrazones

Özlem ATLI¹, Yusuf ÖZKAY^{2,*}

¹Department of Pharmaceutical Toxicology, Faculty of Pharmacy, Anadolu University, Eskişehir, Turkey

²Department of Pharmaceutical Chemistry, Faculty of Pharmacy, Anadolu University, Eskişehir, Turkey

Received: 28.12.2016

Accepted/Published Online: 30.03.2017

Final Version: 10.11.2017

Abstract: A series of new thiazole-hydrazones (**3a–3n**) were synthesized, characterized, and screened for their *h*MAO-A and *h*MAO-B inhibitory activity by an in vitro fluorometric method. Selectivity indexes (SIs) were expressed as IC₅₀ (MAO-A) / IC₅₀ (MAO-B). Compound **3f** showed promising *h*MAO-A inhibition with an IC₅₀ value of 1.20 μM and displayed a very significant SI of 0.04 towards *h*MAO-A. The mechanism of *h*MAO-A inhibition was investigated by enzyme kinetics using Lineweaver–Burk graphics. Compound **3f** was further screened for its cytotoxicity by using a healthy NIH/3T3 mouse embryonic fibroblast cell line (ATCC CRL1658) and was evaluated as nontoxic at its effective concentration against *h*MAO-A. The ADME prediction of the compounds revealed that they may have good pharmacokinetic profiles, which is necessary for drug candidates.

Key words: Thiazole, hydrazone, *h*MAO enzymes, enzyme inhibition

1. Introduction

Monoamine oxidase (MAO) is the key enzyme of brain function, responsible for the metabolism of neurotransmitters by regulating the oxidative deamination of amines in neuronal, glial, and other cells in the brain as well as peripheral tissues.^{1–4} Two main forms of this enzyme are present as MAO-A and MAO-B. MAO-A is mainly present in catecholaminergic neurons of cortex, and MAO-B is found in the serotonergic neurons in the brain.^{3,5} The common substrates for these enzymes are dopamine, tyramine, and tryptamine, whereas serotonin and noradrenaline are particularly metabolized by MAO-A. MAO-B metabolizes small amines like benzylamine and phenethylamine.^{3,5–7} Endogenous amine metabolism results in the formation of toxic reactive oxygen species responsible for oxidative damage and neurodegeneration.^{4,5} Therefore, MAO inhibitors are used for the treatment of neurodegenerative and neurological disorders.^{3,4,8} As the two forms have different substrate selectivities and levels in different regions of brain, their activities are involved in distinct clinical cases.⁴ MAO-B inhibitors are used in multiple therapies for the movement disorders of Parkinson disease and Alzheimer disease,^{4,7,9} whereas MAO-A inhibitors are potent antidepressants and anxiolytic agents.^{3,4,7,8} MAO-A activity has been also found to be associated with neuropsychiatric disorders, including autism, major depressive disorder, and attention deficit hyperactivity disorder.^{4,6} The first-generation irreversible MAO inhibitors were used as antidepressants, but most of these were later withdrawn from the market due to their severe adverse effects. They were reported to cause tachycardia, photophobia, palpitation, nausea, hepatotoxicity, and drug and food interactions. In particular, “tyramine reaction” is a serious health problem from the interaction between the MAO

*Correspondence: yozkay@anadolu.edu.tr

inhibitor and certain foods, and it causes death by manifesting hypertensive crisis.^{7,10} The potentiation effects of MAO-A (not MAO-B) inhibitors on indirectly acting sympathomimetic amines and their minimal tyramine potentiation pointed out the importance of MAO-A inhibitors and led to their reemergence for clinical use in the treatment of depression.¹¹ Since MAO-A is the major enzyme for endogenous amine metabolism, it is the main target of neurological and neurodegenerative disorders commonly caused by this oxidative metabolism.⁶ Thus, design and development of potent and selective MAO-A inhibitors are required because of their features as explained above and the tight involvement of dysregulation of monoamines in neurodegenerative and mental disease development. Reversible and selective MAO-A inhibitory drug development efforts will also lead to the discovery of useful therapeutic agents, which are devoid of unwanted life-threatening adverse effects.^{3,5-7,10}

The development of MAO inhibitors arises from hydrazine derivatives, since the first one developed was the drug iproniazid. Subsequently, heterocyclic hydrazines, hydrazides, and hydrazones were synthesized as potential MAO inhibitors.^{5,12-16} The common structural feature of inhibitors in these studies was an amino or imino group, which seems to play an essential role in orientation and complex formation at the active site of the enzyme¹.

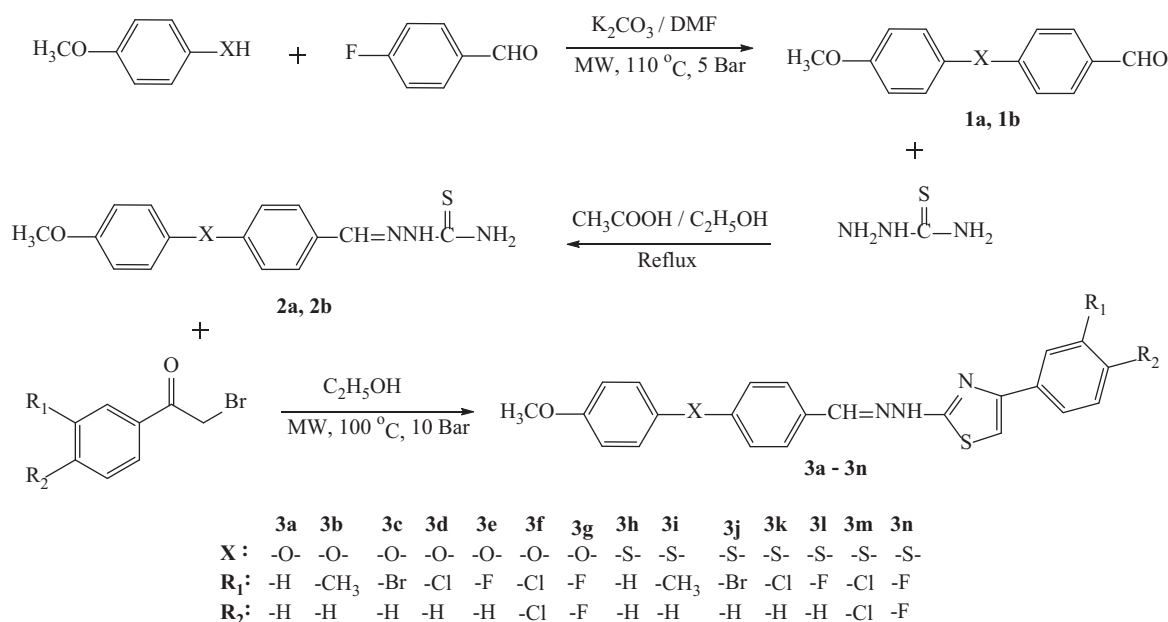
Thiazole was reported as another important heterocyclic moiety for MAO inhibition. From molecular modeling studies, it was found that C4 of the thiazole ring was responsible for the interactions between the inhibitor and the FAD cofactor, which controls the oxidative activity of the MAO enzyme.¹⁰ It was concluded that even a small modification of the substituent's dimension at the C4 position could attenuate the activity of the compound.¹⁰ MAO inhibition potencies of hydrazone and thiazole have directed researchers to synthesize combination products of these two moieties for the development of new MAO inhibitors.^{5,14,17,18} Prompted by this knowledge, in the present study, we synthesized new thiazole-hydrazone compounds to screen their *h*MAO inhibition potency.

2. Results and discussion

2.1. Chemistry

Compounds **3a-3n** were synthesized as outlined in the Scheme. 4-(4-Methoxyphenoxy)benzaldehyde (**1a**) and 4-(4-methoxyphenylsulfanyl)benzaldehyde (**1b**) were prepared under microwave irradiation by reacting 4-fluorobenzaldehyde with 4-methoxyphenol or 4-methoxythiophenol. Compounds **1a** and **1b** were reacted with thiosemicarbazide to gain 4-(4-methoxyphenoxy)benzaldehyde thiosemicarbazone (**2a**) and 4-(4-methoxyphenylsulfanyl)benzaldehyde (**2b**). Hantzsch reaction of compounds **2a** and **2b** with an appropriate α -bromoacetophenone under microwave conditions afforded 4-(4-methoxyphenoxy)benzaldehyde [4-(4-substituted phenyl)-1,3-thiazol-2-yl] hydrazones (**3a-3g**) and 4-(4-methoxyphenylsulfanyl)benzaldehyde [4-(4-substituted phenyl)-1,3-thiazol-2-yl] hydrazones (**3h-3n**) in high yields (88%-96%) and short reaction times (5 min).

Structural elucidation of the synthesized compounds (**3a-3n**) was performed by spectral analyses. The FT-IR spectra of the final products showed characteristic absorption bands at 3155-3346 cm^{-1} for NH and at 1489-1566 cm^{-1} for the azomethine group (CH = N). The ¹H NMR spectra of the compounds showed signals at δ 7.94-8.03 and δ 12.07-12.24 corresponding to the azomethine (CH = N) proton and hydrazide (CONH) proton, respectively. The C5-H proton of the thiazole was observed as a singlet at δ 7.20-7.38. The appearance of a pair of doublets and/or multiplets at δ 6.90-7.90 was due to the aromatic protons of phenyl rings. In the ¹³C NMR spectra, methoxy carbons (OCH₃) were observed at 55.80-55.91 ppm. The carbon of azomethine (CH = N) was assigned at 140.89-141.69 ppm, respectively. The C2 carbon of the thiazole ring appeared at



Scheme. Synthesis pathway for compounds **3a–3n**.

166.75–168.85 ppm. The aromatic carbons were recorded in the region of 103.02–162.05 ppm. Due to the presence of a fluoro substituent in compounds **3e**, **3g**, **3l**, and **3n**, splittings relating to neighboring atoms were detected in the spectra. In the HR-MS spectra of the final compounds (**3a–3n**), the $M + 1$ peak was observed in accordance with their molecular formulas. The $M + 1$ peaks were determined at an accuracy of 2–17 ppm.

2.2. Enzyme inhibition

The synthesized 4-(4-methoxyphenoxy)benzaldehyde [4-(4-substituted phenyl)-1,3-thiazol-2-yl] hydrazones (**3a–3g**) and 4-(4-methoxyphenylsulfanyl)benzaldehyde [4-(4-substituted phenyl)-1,3-thiazol-2-yl] hydrazones (**3h–3n**) were screened for their *h*MAO-A and *h*MAO-B inhibitory activity by an in vitro fluorometric method.^{19,20} The assay is based on the fluorometric detection of H_2O_2 , one of the products generated during the oxidative deamination of the MAO substrate (tyramine), using the OxiRed probe reagent, a highly sensitive and stable probe for H_2O_2 . Clorgiline and selegiline were used as reference drugs. The inhibitory activity results are listed in Table 1.

Against *h*MAO-A, the most active compound **3f** displayed an IC_{50} of 1.20 μM , whereas reference drug clorgiline had an IC_{50} of 0.0071 μM . On the other hand, compound **3f** showed an IC_{50} of 33.47 μM against *h*MAO-B, while reference drug selegiline ($IC_{50} = 0.040 \mu M$) also displayed a significant inhibition against *h*MAO-B. Selectivity indexes (SIs) were expressed as $IC_{50(MAO-A)}/IC_{50(MAO-B)}$. Selectivity towards MAO-A increased as the corresponding SI decreased, while selectivity towards the MAO-B isoform increased as the corresponding SI increased. It was observed that the synthesized compounds have selective inhibition potency against *h*MAO-A. Compound **3f** displayed a very significant SI of 0.04.

In the design of the target compounds (**3a–3n**), the substitution pattern was performed on two regions to discuss the substitution effect on biological activity. The first region shows the difference in terms of 4-(4-methoxyphenoxy) or 4-(4-methoxyphenylsulfanyl) substructures. There is a substituent difference in the second region, which includes the 4-(4-substituted phenyl)-1,3-thiazol substructure. It was observed that compounds

Table 1. IC₅₀ (μM) and selectivity of compounds **3a–3n** against *h*MAO isoforms.

Compound	IC ₅₀ (μM) <i>h</i> MAO-A	IC ₅₀ (μM) <i>h</i> MAO-B	SI	Selectivity
3a	8.54 ± 0.39	50.43 ± 2.48	0.17	MAO-A
3b	12.79 ± 0.58	68.15 ± 3.61	0.19	MAO-A
3c	10.58 ± 0.45	58.40 ± 2.96	0.18	MAO-A
3d	7.72 ± 0.37	39.75 ± 2.73	0.19	MAO-A
3e	9.32 ± 0.51	53.60 ± 3.09	0.17	MAO-A
3f	1.20 ± 0.08	33.47 ± 1.98	0.04	MAO-A
3g	17.62 ± 0.86	58.93 ± 2.54	0.30	MAO-A
3h	26.78 ± 1.73	91.13 ± 4.59	0.29	MAO-A
3i	21.05 ± 1.69	164.17 ± 9.21	0.13	MAO-A
3j	23.06 ± 1.74	95.99 ± 5.47	0.24	MAO-A
3k	21.01 ± 1.91	338.30 ± 14.89	0.06	MAO-A
3l	24.24 ± 1.88	92.21 ± 4.29	0.26	MAO-A
3m	20.71 ± 1.76	69.28 ± 3.75	0.30	MAO-A
3n	26.74 ± 1.53	279.70 ± 13.27	0.10	MAO-A
Clorgiline	0.0071 ± 0.0004	-	-	MAO-A
Selegiline	-	0.044 ± 0.003	-	MAO-B

3a–3g have more potency to inhibit the MAO enzymes when compared to compounds **3h–3n**. This result suggests that the first structural region has an impact on enzyme inhibition, and it may be declared that the presence of oxygen instead of sulfur enhances the enzyme inhibitory activity. The substituent change in the second structural region also has an effect on enzyme inhibitory activity. Among compounds **3a–3g**, compound **3f** has a higher potency to inhibit the MAO enzymes, which may be the result of a more lipophilic character due to dichloro substitution.

2.3. Kinetic studies of enzyme inhibition

The mechanism of *h*MAO-A inhibition was investigated by enzyme kinetics, following a procedure similar to the MAO inhibition assay. The linear Lineweaver–Burk graphics were used to estimate the type of inhibition.²¹ The enzyme was analyzed by recording substrate-velocity curves in the absence and presence of the most potent compound, **3f**, which was prepared at concentrations of IC₅₀ / 4 (0.30 μM), IC₅₀ / 2 (0.60 μM), IC₅₀ (1.20 μM), 2 × IC₅₀ (2.40 μM), and 4 × IC₅₀ (4.80 μM) (Figures 1A and 1B). In each case, the initial velocity measurements were gained at different substrate (tyramine) concentrations ranging from 20 μM to 0.625 μM. Replots of the slopes of the Lineweaver–Burk plots versus inhibitor concentration are presented in Figure 1. The Lineweaver–Burk plot introduces the inhibition type as mixed type, competitive or noncompetitive. In mixed-typed inhibition, the lines cross neither the x- nor the y-axis at the same point. Noncompetitive inhibition has plots with the same intercept on the x-axis, but there are different slopes and intercepts on the y-axis. Competitive inhibitors possess the same intercept on the y-axis, but there are diverse slopes and intercepts on the x-axis between the two datasets, as seen in Figure 1. Therefore, this pattern indicates that the mechanism of *h*MAO-A inhibition of **3f** is competitive, explaining that the inhibitor can bind to the enzyme in competition with the substrate. The K_i value for compound **3f** was calculated as 1.453 μM for the inhibition of *h*MAO-A.

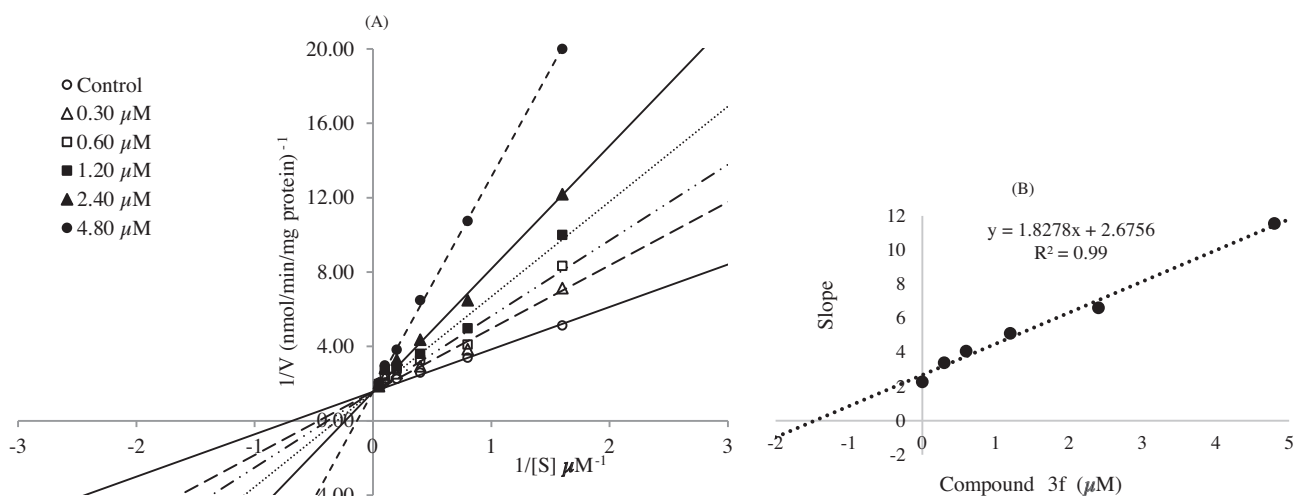


Figure. A) Lineweaver–Burk plots for the inhibition of *h*MAO-A by compound **3f**. [S], substrate concentration [μM]; V, reaction velocity [$\text{nmol min}^{-1} \text{mg}^{-1}$]. Inhibitor concentrations are shown on the left. V_{max} value for competitive inhibition was calculated as 0.6410. Respective K_m values from 4.80 μM to control: 7.411, 4.242, 3.280, 2.611, 2.181, 1.463 μM . B) Replots of the slopes of the Lineweaver–Burk plots versus inhibitor concentration. K_i was calculated as 1.453 μM .

2.4. Cytotoxicity test

The toxicity of compound **3f** was investigated by MTT assay, which is based on the reduction of yellow MTT dye by metabolically active eukaryotic and prokaryotic cells to form the purple formazan product. This assay is mainly preferred to establish an understanding about cell viability and to observe the growth of cell cultures.^{22,23} MTT assay was carried out using the healthy NIH/3T3 mouse embryonic fibroblast cell line (ATCC CRL1658), which is recommended for cytotoxicity screening by ISO 10993-5.²⁴ As seen in Table 2, the IC_{50} values of the reference drugs and **3f** against NIH/3T3 cells were found to be ≥ 1000 μM , which is significantly higher than their IC_{50} values against *h*MAO enzymes. Thus, it can be stated that compound **3f** is nontoxic at its effective concentration against *h*MAO-A.

Table 2. IC_{50} (μM) values of the reference drugs and **3f** against the NIH/3T3 cell line.

Compound	Clorgiline	Selegiline	3f
IC_{50} (μM)	≥ 1000	≥ 1000	≥ 1000

2.5. Theoretical prediction of ADME properties and BBB permeability

Essential pharmacological activity and low toxicological effects are not adequate for a compound to become a drug candidate. A good pharmacokinetics profile is also very important for new drug candidates and should be assessed earlier in the process of drug development. In recent years, noteworthy developments in combinatorial chemistry have made the estimation of absorption, distribution, metabolism, and excretion (ADME) relatively easy.²⁵ The theoretical calculation of the ADME properties (molecular weight, log P, tPSA, number of hydrogen donors and acceptors, volume) of compounds (**3a–3n**) was carried out and this is presented in Table 3 along with violations of Lipinski's rule.²⁶ This rule suggests that an orally active drug should not have more than one violation. According to the findings in Table 3, all compounds obey Lipinski's rule. On the other hand, all

calculated physicochemical parameters for compound **3f** are compatible with Lipinski's rule except the log P value. Although the log P (7.05) of compound **3f** exceeds Lipinski's limit, it shows that the related compound has a lipophilic character, which is suitable to cross the central nervous system (CNS). Furthermore, tPSA, described to be a predictive indicator of membrane penetration, is positive (55.75), and as MAO inhibitors have to pass different membranes and reach the CNS, this supports the potential of compound **3f**.²⁷

Table 3. Some physicochemical parameters of the compounds **3a–3n** and reference drugs used in the prediction of ADME profiles.

Comp.	MW	logP	tPSA	nON	nOHNH	MV	Vio	BBB (+ / -)
3a	401.49	5.77	55.75	5	1	355.02	1	+
3b	415.52	6.22	55.75	5	1	371.58	1	+
3c	480.39	6.58	55.75	5	1	372.90	1	+
3d	435.94	6.45	55.75	5	1	368.55	1	+
3e	419.48	5.93	55.75	5	1	359.95	1	+
3f	470.38	7.05	55.75	5	1	382.09	1	+
3g	437.47	6.02	55.75	5	1	364.88	1	+
3h	417.56	5.98	46.52	5	1	364.16	1	+
3i	431.59	6.43	46.52	5	1	380.72	1	+
3j	496.45	6.79	46.52	5	1	382.05	1	+
3k	452.00	6.66	46.52	5	1	377.70	1	+
3l	435.55	6.14	46.52	5	1	369.09	1	+
3m	486.45	7.26	46.52	5	1	391.23	1	+
3n	453.54	6.24	46.52	5	1	374.02	1	+
Selegiline	187.29	2.64	3.24	1	0	202.64	0	+
Clorgiline	272.18	3.74	12.47	2	0	238.91	0	+

MW: Molecular weight; log P: log octanol/water partition coefficient; tPSA: total polar surface area; nON: number of hydrogen acceptors; nOHNH: number of hydrogen donors; MV: molecular volume; Vio: violations of Lipinski's rule were calculated using the Molinspiration Calculation of Molecular Properties toolkit. BBB (+ / -): Blood–brain barrier permeability was calculated with the CBLigand BBB prediction server.

Drugs that specifically target the CNS must first pass the blood–brain barrier (BBB). Although the BBB is protective in nature, the inability of drug molecules to permeate the BBB is a significant impediment for CNS drug candidates and should be addressed early in the drug discovery process. Thus, the task of predicting the BBB permeability of new compounds is of great importance.²⁸ From this point of view, BBB permeability of the synthesized compounds (**3a–3n**) was calculated by the CBLigand BBB prediction server (<http://www.cbligand.org/BBB/index.php>). This predictor uses two different algorithms, AdaBoost and support vector machine (SVM), combined with four different fingerprints to predict if a compound can pass (+) or cannot pass (-) the BBB. In each case, the predictor generates scores higher than 0 if the compound can pass the BBB. As presented in Table 3, all calculations for the synthesized compounds resulted in BBB (+), which is necessary for MAO inhibitors.

2.6. Conclusions

In summary, preliminary evaluation of new 4-(4-methoxyphenoxy)benzaldehyde [4-(4-substituted phenyl)-1,3-thiazol-2-yl] hydrazones (**3a–3g**) and 4-(4-methoxyphenylsulfanyl)benzaldehyde [4-(4-substituted phenyl)-1,3-thiazol-2-yl] hydrazones (**3h–3n**) as *h*MAO inhibitory agents resulted in promising findings. Compound **3f**

displayed good *h*MAO-A inhibition. Furthermore, this compound did not show any cytotoxicity. Consequently, the findings of the present study will not only direct our research group to further studies but may also encourage medicinal chemists to synthesize more effective and safer compounds bearing chemical structures similar to those of compound **3f**.

3. Experimental

3.1. Chemistry

All chemicals were purchased from Sigma Aldrich Chemicals (Sigma Aldrich Corp., St. Louis, MO, USA) and Merck Chemicals (Merck KGaA, Darmstadt, Germany). All melting points (mp) were determined with an MP90 digital melting point apparatus (Mettler Toledo, Columbus, OH, USA) and were uncorrected. All reactions were monitored by thin-layer chromatography (TLC) using silica gel 60 F254 TLC plates (Merck KGaA, Darmstadt, Germany). Spectroscopic data were recorded with the following instruments: IR, Shimadzu Affinity 1S spectrophotometer (Shimadzu, Tokyo, Japan); NMR, Bruker DPX 300 NMR spectrometer (Bruker Bioscience, Billerica, MA, USA), in DMSO-*d*₆, using TMS as internal standard; M + 1 peaks, Shimadzu LC/MS IT-TOF system (Shimadzu).

3.2. Synthesis of 4-(4-methoxyphenoxy)benzaldehyde (**1a**) and 4-(4-methoxyphenylsulfanyl)benzaldehyde (**1b**)

A mixture of 4-fluorobenzaldehyde (40 mmol, 4.28 mL), 4-methoxyphenol (40 mmol, 4.96 g), or 4-methoxythiophenol (40 mmol, 4.92 mL) and dimethylformamide (DMF) (10 mL) were added into a vial (30 mL) of microwave synthesis reactor (Anton-Paar, Monowave 300, Austria). The reaction mixture was heated under conditions of 110 °C and 5 bar for 15 min. After cooling, the mixture was poured into ice water and the precipitated product was washed with water, dried, and recrystallized from ethanol to give 4-(4-methoxyphenoxy)benzaldehyde (**1a**) at yield: 92%; mp: 61 °C; ref. mp: 60 °C²⁹ and 4-(4-methoxyphenylsulfanyl)benzaldehyde (**1b**) at yield: 94%; mp: 46 °C; ref. mp: 46–46.5 °C³⁰.

3.3. Synthesis of 4-(4-methoxyphenoxy)benzaldehyde thiosemicarbazone (**2a**) and 4-(4-methoxyphenylsulfanyl)benzaldehyde (**2b**)

A mixture of thiosemicarbazide (30 mmol, 2.7 g) and compound **1a** (30 mmol, 6.84 g) or **1b** (30 mmol, 7.32 g) in ethanol (20 mL) was refluxed for 2 h. The progress of the reaction was monitored by TLC. The resulting mixture was cooled, poured into ice water, filtered, and then recrystallized from ethanol to afford 4-(4-methoxyphenoxy)benzaldehyde thiosemicarbazone (**2a**) at yield: 86%; mp: 175 °C; ref. mp: 174 °C³¹ and 4-(4-methoxyphenylsulfanyl)benzaldehyde thiosemicarbazone (**2b**) at yield: 88%, mp: 165.3 °C, FTIR (ATR, cm⁻¹): 3414 (N - H), 3282 (N - H), 3149 (N - H), 1487 (C = N), 1274 (C - N), 815, 804. ¹H NMR (300 MHz, DMSO-*d*₆): δ = 3.79 (3H, s, OCH₃), 7.03 (2H, d, *J* = 8.80 Hz, methoxyphenyl H_{3,3'}), 7.07 (2H, d, *J* = 8.40 Hz, benzyldene H_{2,2'}), 7.45 (2H, d, *J* = 8.80 Hz, methoxyphenyl H_{2,2'}), 7.70 (2H, d, *J* = 8.40 Hz, benzyldene H_{3,3'}), 7.95 (1H, br, NH₂), 7.97 (1H, s, azomethine CH), 8.18 (1H, br, NH₂), 11.41 (1H, s, NH). ¹³C NMR (75 MHz, DMSO-*d*₆): δ = 55.83 (OCH₃), 115.99 (methoxyphenyl C_{3,3'}), 122.28 (methoxyphenyl C₁), 127.37 (methoxyphenyl C_{2,2'}), 128.42 (benzyldene C_{2,2'}), 132.19 (benzyldene C₁), 136.37 (benzyldene

C_{3,3'}), 140.92 (benzylidene C₄), 141.94 (C = N), 160.50 (methoxyphenyl C₄), 178.33 (C = S). HRMS (m / z): [M + H]⁺ calcd for C₁₅H₁₅N₃OS₂: 318.0729; found: 318.0721.

3.4. Synthesis of 4-(4-methoxyphenoxy)benzaldehyde [4-(4-substituted phenyl)-1,3-thiazol-2-yl] hydrazones (3a–3g) and 4-(4-methoxyphenylsulfanyl)benzaldehyde [4-(4-substituted phenyl)-1,3-thiazol-2-yl] hydrazones (3h–3n)

A mixture of appropriate α -bromoacetophenone (2 mmol) and compound **2a** (2 mmol, 0.600 g) or **2b** (2 mmol, 0.632 g) in ethanol (10 mL) was added to a vial (30 mL) of microwave synthesis reactor (Anton-Paar, Monowave 300). The reaction mixture was heated under conditions of 100 °C and 10 bar for 5 min. After cooling, the mixture was poured into ice water and the precipitated product was washed with water, dried, and recrystallized from ethanol to give 4-(4-methoxyphenoxy)benzaldehyde [4-(4-substituted phenyl)-1,3-thiazol-2-yl] hydrazones (**3a–3g**) and 4-(4-methoxyphenylsulfanyl)benzaldehyde [4-(4-substituted phenyl)-1,3-thiazol-2-yl] hydrazones (**3h–3n**).

3.4.1. 4-(4-Methoxyphenoxy)benzaldehyde (4-phenyl-1,3-thiazol-2-yl) hydrazone (3a)

Yield: 89%, mp = 203.3 °C, FTIR (ATR, cm⁻¹): 3169 (N - H), 1494 (C = N), 1222 (C - N), 827, 707. ¹H NMR (300 MHz, DMSO-*d*₆): δ = 3.76 (3H, s, OCH₃), 6.96 (2H, d, *J* = 8.58 Hz, methoxyphenyl H_{3,3'}), 7.00–7.07 (4H, m, methoxyphenyl H_{2,2'}, benzylidene H_{2,2'}), 7.29–7.31 (2H, m, monosubstituted phenyl H₄, thiazole H), 7.40 (2H, t, *J* = 7.32 Hz, monosubstituted phenyl H_{3,3'}), 7.63 (2H, d, *J* = 8.73 Hz, benzylidene H_{2,2'}), 7.85 (2H, d, *J* = 7.32 Hz, monosubstituted phenyl H_{2,2'}), 8.00 (1H, s, azomethine CH), 12.09 (1H, s, NH). ¹³C NMR (75 MHz, DMSO-*d*₆): δ = 55.88 (OCH₃), 103.97 (thiazole C₅), 115.64 (methoxyphenyl C_{3,3'}), 117.77 (benzylidene C₁), 121.55 (benzylidene C_{3,3'}), 125.96 (monosubstituted phenyl C₄), 127.97 (methoxyphenyl C_{2,2'}), 128.45 (monosubstituted phenyl C_{3,3'}), 129.06 (monosubstituted phenyl C_{2,2'}), 129.29 (benzylidene C_{2,2'}), 135.17 (monosubstituted phenyl C₁), 141.22 (C = N), 149.22 (methoxyphenyl C₁), 151.16 (thiazole C₄), 156.41 (benzylidene C₄), 159.52 (methoxyphenyl C₄), 168.70 (thiazole C₂). HRMS (m / z): [M + H]⁺ calcd for C₂₃H₁₉N₃O₂S: 402.1271; found: 402.1265.

3.4.2. 4-(4-Methoxyphenoxy)benzaldehyde [4-(4-methylphenyl)-1,3-thiazol-2-yl] hydrazone (3b)

Yield: 92%, mp = 131.3 °C, FTIR (ATR, cm⁻¹): 3302 (N - H), 1496 (C = N), 1228 (C - N), 839, 727. ¹H NMR (300 MHz, DMSO-*d*₆): δ = 2.32 (3H, s, CH₃), 3.77 (3H, s, OCH₃), 6.95–7.03 (4H, m, benzylidene H_{2,2'}, methoxyphenyl H_{3,3'}), 7.06 (2H, d, *J* = 9.21 Hz, methoxyphenyl H_{2,2'}), 7.20–7.25 (3H, m, methylphenyl H_{3,3'}, thiazole H), 7.63 (2H, d, *J* = 8.85 Hz, benzylidene H_{3,3'}), 7.74 (2H, d, *J* = 8.13 Hz, methylphenyl H_{2,2'}), 8.00 (1H, s, azomethine CH), 12.07 (1H, s, NH). ¹³C NMR (75 MHz, DMSO-*d*₆): δ = 21.26 (CH₃), 55.89 (OCH₃), 103.02 (thiazole C₅), 115.62 (methoxyphenyl C_{3,3'}), 117.76 (benzylidene C₁), 121.54 (benzylidene C_{3,3'}), 125.91 (methylphenyl C₄), 128.43 (methoxyphenyl C_{2,2'}), 129.31 (benzylidene C_{2,2'}), 129.62 (methylphenyl C₄), 132.50 (methylphenyl C_{2,2'}), 137.23 (methylphenyl C₁), 141.19 (C = N), 149.21 (methoxyphenyl C₁), 150.97 (thiazole C₄), 156.40 (benzylidene C₄), 159.50 (methoxyphenyl C₄), 168.61 (thiazole C₂). HRMS (m / z): [M + H]⁺ calcd for C₂₄H₂₁N₃O₂S: 416.1427; found: 416.1417.

3.4.3. 4-(4-Methoxyphenoxy)benzaldehyde [4-(4-bromophenyl)-1,3-thiazol-2-yl] hydrazone (3c)

Yield: 89%, mp = 208.5 °C, FTIR (ATR, cm^{-1}): 3305 (N - H), 1496 (C = N), 1230 (C - N), 1051, 839, 729. ^1H NMR (300 MHz, DMSO- d_6): δ = 3.76 (3H, s, OCH_3), 6.94–6.99 (4H, m, benzyldiene $\text{H}_{2,2'}$, methoxyphenyl $\text{H}_{3,3'}$), 7.06 (2H, d, J = 9.18 Hz, methoxyphenyl $\text{H}_{2,2'}$), 7.38 (1H, s, thiazole H), 7.59 (2H, d, J = 8.58 Hz, bromophenyl $\text{H}_{2,2'}$), 7.63 (2H, d, J = 8.82 Hz, benzyldiene $\text{H}_{3,3'}$), 7.80 (2H, d, J = 8.58 Hz, bromophenyl $\text{H}_{3,3'}$), 8.00 (1H, s, azomethine CH), 12.10 (1H, s, NH). ^{13}C NMR (75 MHz, DMSO- d_6): δ = 55.88 (OCH_3), 104.87 (thiazole C_5), 115.63 (methoxyphenyl $\text{C}_{3,3'}$), 117.76 (benzyldiene C_1), 120.95 (bromophenyl C_1), 121.55 (benzyldiene $\text{C}_{3,3'}$), 127.99 (methoxyphenyl $\text{C}_{2,2'}$), 128.49 (bromophenyl $\text{C}_{2,2'}$), 129.22 (benzyldiene $\text{C}_{2,2'}$), 131.99 (bromophenyl $\text{C}_{3,3'}$), 134.37 (bromophenyl C_4), 141.45 (C = N), 149.20 (methoxyphenyl C_1), 149.81 (thiazole C_4), 156.41 (benzyldiene C_4), 159.56 (methoxyphenyl C_4), 168.85 (thiazole C_2). HRMS (m / z): $[\text{M} + \text{H}]^+$ calcd for $\text{C}_{23}\text{H}_{18}\text{BrN}_3\text{O}_2\text{S}$: 480.0376; found: 480.0360.

3.4.4. 4-(4-Methoxyphenoxy)benzaldehyde [4-(4-chlorophenyl)-1,3-thiazol-2-yl] hydrazone (3d)

Yield: 93%, mp = 192.9 °C, FTIR (ATR, cm^{-1}): 3305 (N - H), 1504 (C = N), 1244 (C - N), 839, 731. ^1H NMR (300 MHz, DMSO- d_6): δ = 3.76 (3H, s, OCH_3), 6.96 (2H, d, J = 8.61 Hz, methoxyphenyl $\text{H}_{3,3'}$), 6.99–7.07 (4H, m, benzyldiene $\text{H}_{2,2'}$, methoxyphenyl $\text{H}_{2,2'}$), 7.37 (1H, s, thiazole H), 7.46 (2H, d, J = 8.61 Hz, chlorophenyl $\text{H}_{2,2'}$), 7.63 (2H, d, J = 8.79 Hz, benzyldiene $\text{H}_{3,3'}$), 7.86 (2H, d, J = 8.58 Hz, chlorophenyl $\text{H}_{3,3'}$), 8.00 (1H, s, azomethine CH), 12.09 (1H, s, NH). ^{13}C NMR (75 MHz, DMSO- d_6): δ = 55.91 (OCH_3), 104.79 (thiazole C_5), 115.64 (methoxyphenyl $\text{C}_{3,3'}$), 117.76 (benzyldiene C_1), 121.55 (benzyldiene $\text{C}_{3,3'}$), 127.67 (methoxyphenyl $\text{C}_{2,2'}$), 128.48 (chlorophenyl C_1), 129.08 (benzyldiene $\text{C}_{2,2'}$), 129.23 (chlorophenyl $\text{C}_{2,2'}$), 132.35 (chlorophenyl $\text{C}_{3,3'}$), 134.03 (chlorophenyl C_4), 141.42 (C = N), 149.20 (methoxyphenyl C_1), 149.79 (thiazole C_4), 156.41 (benzyldiene C_4), 159.56 (methoxyphenyl C_4), 168.84 (thiazole C_2). HRMS (m / z): $[\text{M} + \text{H}]^+$ calcd for $\text{C}_{23}\text{H}_{18}\text{ClN}_3\text{O}_2\text{S}$: 436.0881; found: 436.0874.

3.4.5. 4-(4-Methoxyphenoxy)benzaldehyde [4-(4-fluorophenyl)-1,3-thiazol-2-yl] hydrazone (3e)

Yield: 91%, mp = 224.9 °C, FTIR (ATR, cm^{-1}): 3305 (N - H), 1496 (C = N), 1226 (C - N), 842, 827. ^1H NMR (300 MHz, DMSO- d_6): δ = 3.75 (3H, s, OCH_3), 6.90–7.06 (6H, m, benzyldiene $\text{H}_{2,2'}$, methoxyphenyl $\text{H}_{2,3,2',3'}$), 7.21 (3H, m, fluorophenyl $\text{H}_{2,2'}$, thiazole), 7.62 (2H, d, J = 8.79 Hz, benzyldiene $\text{H}_{3,3'}$), 7.88 (2H, d, J = 8.82 Hz, fluorophenyl $\text{H}_{3,3'}$), 8.00 (1H, s, azomethine CH), 12.09 (1H, s, NH). ^{13}C NMR (75 MHz, DMSO- d_6): δ = 55.87 (OCH_3), 103.69 (thiazole C_5), 115.74 (methoxyphenyl $\text{C}_{3,3'}$), 117.75 (benzyldiene C_1), 121.54 (benzyldiene $\text{C}_{3,3'}$), 127.93 ($J_{\text{CF}-3}$ = 8.05 Hz, fluorophenyl $\text{C}_{2,2'}$), 128.46 (methoxyphenyl $\text{C}_{2,2'}$), 128.99 (fluorophenyl C_1), 129.08 (benzyldiene $\text{C}_{2,2'}$), 129.45 ($J_{\text{CF}-2}$ = 27.14 Hz, fluorophenyl $\text{C}_{3,3'}$), 131.78, 141.34 (C = N), 146.41 (thiazole C_4), 149.20 (methoxyphenyl C_1), 156.40 (benzyldiene C_4), 159.43 (methoxyphenyl C_4), 162.05 ($J_{\text{CF}-1}$ = 242.71 Hz, fluorophenyl C_4), 168.82 (thiazole C_2). HRMS (m / z): $[\text{M} + \text{H}]^+$ calcd for $\text{C}_{23}\text{H}_{18}\text{FN}_3\text{O}_2\text{S}$: 420.1170; found: 419.1182.

3.4.6. 4-(4-Methoxyphenoxy)benzaldehyde [4-(2,4-dichlorophenyl)-1,3-thiazol-2-yl] hydrazone (3f)

Yield: 89%, mp = 190.1 °C, FTIR (ATR, cm^{-1}): 3157 (N - H), 1494 (C = N), 1230 (C - N), 827, 738. ^1H NMR (300 MHz, DMSO- d_6): δ = 3.76 (3H, s, OCH_3), 6.94–6.97 (2H, d, J = 8.82 Hz, benzyldiene $\text{H}_{2,2'}$), 6.97–7.06 (4H, m, methoxyphenyl $\text{H}_{2,3,2',3'}$), 7.38 (1H, s, thiazole H), 7.49 (1H, dd, J = 2.22–8.52 Hz, dichlorophenyl

H₅), 7.63 (2H, d, $J = 8.82$ Hz, benzyldiene H_{3,3'}), 7.68 (1H, d, $J = 2.16$ Hz, dichlorophenyl H₃), 7.89 (1H, d, $J = 8.52$ Hz, dichlorophenyl H₆), 8.01 (1H, s, azomethine CH), 12.11 (1H, s, NH). ¹³C NMR (75 MHz, DMSO-*d*₆): $\delta = 55.90$ (OCH₃), 109.53 (thiazole C₅), 115.63 (methoxyphenyl C_{3,3'}), 117.77 (benzyldiene C₁), 121.54 (benzyldiene C_{3,3'}), 127.95 (methoxyphenyl C_{2,2'}), 128.50 (benzyldiene C_{2,2'}), 129.21 (dichlorophenyl C₃), 130.22 (dichlorophenyl C₅), 132.00 (dichlorophenyl C₁), 132.63 (dichlorophenyl C₆), 132.66 (dichlorophenyl C₄), 132.91 (dichlorophenyl C₂), 141.52 (C = N), 146.38 (thiazole C₄), 149.20 (methoxyphenyl C₁), 156.41 (benzyldiene C₄), 159.58 (methoxyphenyl C₄), 167.94 (thiazole C₂). HRMS (*m/z*): [M + H]⁺ calcd for C₂₃H₁₇Cl₂N₃O₂S: 470.0491; found: 470.0474.

3.4.7. 4-(4-Methoxyphenoxy)benzaldehyde [4-(2,4-difluorophenyl)-1,3-thiazol-2-yl] hydrazone (3g)

Yield: 95%, mp = 146.1 °C, FTIR (ATR, cm⁻¹): 3346 (N - H), 1496 (C = N), 1222 (C - N), 831, 742. ¹H NMR (300 MHz, DMSO-*d*₆): $\delta = 3.76$ (3H, s, OCH₃), 6.96 (2H, d, $J = 8.34$ Hz, methoxyphenyl H_{3,3'}), 6.99–7.07 (4H, m, benzyldiene H_{2,2'}, methoxyphenyl H_{2,2'}), 7.14–7.20 (2H, m, difluorophenyl H₅, thiazole H), 7.30–7.37 (1H, m, difluorophenyl H₃), 7.63 (2H, d, $J = 8.73$ Hz, benzyldiene H_{3,3'}), 8.00–8.03 (2H, m, azomethine CH, difluorophenyl H₆), 12.15 (1H, s, NH). ¹³C NMR (75 MHz, DMSO-*d*₆): $\delta = 55.90$ (OCH₃), 104.70 (t, $J = 26.3$ Hz, difluorophenyl C₃), 108.11 (d, $J = 13.8$ Hz, thiazole C₄), 112.30 (dd, $J = 2.8$ –21.0 Hz, difluorophenyl C₅), 115.63 (methoxyphenyl C_{3,3'}), 117.75 (benzyldiene C₁), 119.51 (dd, $J = 3.9$ –11.2 Hz, difluorophenyl C₁), 121.56 (benzyldiene C_{3,3'}), 128.52 (methoxyphenyl C_{2,2'}), 129.18 (benzyldiene C_{2,2'}), 130.87 (dd, $J = 4.2$ –10.2 Hz, difluorophenyl C₆), 141.69 (C = N), 143.63 (thiazole C₄), 149.18 (methoxyphenyl C₁), 156.41 (benzyldiene C₄), 159.60 (methoxyphenyl C₄), 160.07 (dd, $J = 12.0$ –250.3 Hz, difluorophenyl C₄), 161.75 (dd, $J = 12.6$ –245.7 Hz, difluorophenyl C₂), 168.19 (thiazole C₂). HRMS (*m/z*): [M + H]⁺ calcd for C₂₃H₁₇F₂N₃O₂S: 438.1082; found: 438.1078

3.4.8. 4-(4-Methoxyphenylsulfanyl)benzaldehyde (4-phenyl-1,3-thiazol-2-yl) hydrazone (3h)

Yield: 96%, mp = 162.9 °C, FTIR (ATR, cm⁻¹): 3313 (N - H), 1566 (C = N), 1242 (C - N), 823, 711. ¹H NMR (300 MHz, DMSO-*d*₆): $\delta = 3.80$ (3H, s, OCH₃), 7.04 (2H, d, $J = 8.58$ Hz, methoxyphenyl H_{3,3'}), 7.00–7.07 (4H, m, benzyldiene H_{3,3'}, methoxyphenyl H_{2,2'}), 7.38–7.40 (2H, m, monosubstituted phenyl H₄, thiazole H), 7.46 (2H, d, $J = 8.85$ Hz, monosubstituted phenyl H_{3,3'}), 7.63 (2H, d, $J = 8.49$ Hz, benzyldiene H_{2,2'}), 7.83–7.86 (2H, m, monosubstituted phenyl H_{2,2'}), 7.96 (1H, s, azomethine CH), 12.17 (1H, s, NH). ¹³C NMR (75 MHz, DMSO-*d*₆): $\delta = 55.81$ (OCH₃), 104.15 (thiazole C₅), 115.99 (methoxyphenyl C_{3,3'}), 125.96 (methoxyphenyl C₁), 127.41 (monosubstituted phenyl C₄), 127.85 (methoxyphenyl C_{2,2'}), 128.26 (benzyldiene C_{2,2'}), 128.72 (monosubstituted phenyl C_{3,3'}), 129.07 (monosubstituted phenyl C_{2,2'}), 132.47 (benzyldiene C₁), 135.97 (monosubstituted phenyl C₁), 136.16 (benzyldiene C_{3,3'}), 140.03 (benzyldiene C₄), 141.00 (C = N), 148.46 (thiazole C₄), 160.15 (methoxyphenyl C₄), 168.21 (thiazole C₂). HRMS (*m/z*): [M + H]⁺ calcd for C₂₃H₁₉N₃OS₂: 418.1042; found: 418.1038.

3.4.9. 4-(4-Methoxyphenylsulfanyl)benzaldehyde [4-(4-methylphenyl)-1,3-thiazol-2-yl] hydrazone (3i)

Yield: 93 %, mp = 179.7 °C, FTIR (ATR, cm⁻¹): 3155 (N - H), 1489 (C = N), 1246 (C - N), 815, 727. ¹H NMR (300 MHz, DMSO-*d*₆): $\delta = 2.31$ (3H, s, CH₃), 3.80 (3H, s, OCH₃), 7.04 (2H, d, $J = 8.82$ Hz, methoxyphenyl H_{3,3'}), 7.13 (2H, d, $J = 8.40$ Hz, benzyldiene H_{2,2'}), 7.19 (2H, d, $J = 8.13$ Hz, methylphenyl H_{3,3'}), 7.23 (1H, s, thiazole H), 7.46 (2H, d, $J = 8.79$ Hz, methoxyphenyl H_{2,2'}), 7.56 (2H, d, $J = 8.46$ Hz, benzyldiene H_{3,3'}), 7.73

(2H, d, $J = 8.13$ Hz, methylphenyl $H_{2,2'}$), 7.95 (1H, s, azomethine CH), 12.13 (1H, s, NH). ^{13}C NMR (75 MHz, DMSO- d_6): $\delta = 21.28$ (CH_3), 55.82 (OCH_3), 103.23 (thiazole C_5), 115.98 (methoxyphenyl $\text{C}_{3,3'}$), 122.53 (methoxyphenyl C_1), 125.91 (methylphenyl $\text{C}_{3,3'}$), 127.39 (methylphenyl C_4), 127.86 (methoxyphenyl $\text{C}_{2,2'}$), 129.63 (benzylidene $\text{C}_{2,2'}$), 132.50 (benzylidene C_1), 136.21 (methylphenyl $\text{C}_{2,2'}$), 137.25 (methylphenyl C_1), 139.99 (benzylidene C_4), 140.89 ($\text{C} = \text{N}$), 148.29 (thiazole C_4), 160.43 (methoxyphenyl C_4), 168.47 (thiazole C_2). HRMS (m/z): $[\text{M} + \text{H}]^+$ calcd for $\text{C}_{24}\text{H}_{21}\text{N}_3\text{OS}_2$: 432.1199; found: 432.1191.

3.4.10. 4-(4-Methoxyphenylsulfanyl)benzaldehyde [4-(4-bromophenyl)-1,3-thiazol-2-yl] hydrazone (3j)

Yield: 88%, mp = 205.7 °C, FTIR (ATR, cm^{-1}): 3159 (N - H), 1489 ($\text{C} = \text{N}$), 1247 ($\text{C} - \text{N}$), 819, 725. ^1H NMR (300 MHz, DMSO- d_6): $\delta = 3.79$ (3H, s, OCH_3), 7.03 (2H, d, $J = 8.79$ Hz, methoxyphenyl $\text{H}_{3,3'}$), 7.13 (2H, d, $J = 8.40$ Hz, benzylidene $\text{H}_{2,2'}$), 7.38 (1H, s, thiazole H), 7.45 (2H, d, $J = 8.76$ Hz, methoxyphenyl $\text{H}_{2,2'}$), 7.54–7.60 (4H, m, benzylidene $\text{H}_{3,3'}$, bromophenyl $\text{H}_{2,2'}$), 7.79 (2H, d, $J = 8.55$ Hz, bromophenyl $\text{H}_{3,3'}$), 7.96 (1H, s, azomethine CH), 12.17 (1H, s, NH). ^{13}C NMR (75 MHz, DMSO- d_6): $\delta = 55.82$ (OCH_3), 105.06 (thiazole C_5), 115.97 (methoxyphenyl $\text{C}_{3,3'}$), 120.98 (bromophenyl C_1), 122.50 (methoxyphenyl C_1), 127.43 (bromophenyl $\text{C}_{2,2'}$), 127.82 (methoxyphenyl $\text{C}_{2,2'}$), 127.98 (benzylidene $\text{C}_{2,2'}$), 131.99 (bromophenyl $\text{C}_{3,3'}$), 132.40 (benzylidene C_1), 134.33 (bromophenyl C_4), 136.23 (benzylidene $\text{C}_{3,3'}$), 140.13 (benzylidene C_4), 141.18 ($\text{C} = \text{N}$), 149.82 (thiazole C_4), 160.44 (methoxyphenyl C_4), 168.73 (thiazole C_2). HRMS (m/z): $[\text{M} + \text{H}]^+$ calcd for $\text{C}_{23}\text{H}_{18}\text{BrN}_3\text{OS}_2$: 496.0147; found: 496.0131.

3.4.11. 4-(4-Methoxyphenylsulfanyl)benzaldehyde [4-(4-chlorophenyl)-1,3-thiazol-2-yl] hydrazone (3k)

Yield: 90%, mp = 196.4 °C, FTIR (ATR, cm^{-1}): 3205 (N - H), 1489 ($\text{C} = \text{N}$), 1247 ($\text{C} - \text{N}$), 821, 725. ^1H NMR (300 MHz, DMSO- d_6): $\delta = 3.79$ (3H, s, OCH_3), 7.03 (2H, d, $J = 8.76$ Hz, methoxyphenyl $\text{H}_{3,3'}$), 7.13 (2H, d, $J = 8.37$ Hz, benzylidene $\text{H}_{2,2'}$), 7.37 (1H, s, thiazole H), 7.44–7.46 (4H, m, methoxyphenyl $\text{H}_{3,3'}$, chlorophenyl $\text{H}_{2,2'}$), 7.56 (2H, d, $J = 8.43$ Hz, benzylidene $\text{H}_{3,3'}$), 7.86 (2H, d, $J = 8.55$ Hz, chlorophenyl $\text{H}_{3,3'}$), 7.96 (1H, s, azomethine CH), 12.17 (1H, s, NH). ^{13}C NMR (75 MHz, DMSO- d_6): $\delta = 55.82$ (OCH_3), 104.96 (thiazole C_5), 115.97 (methoxyphenyl $\text{C}_{3,3'}$), 122.50 (methoxyphenyl C_1), 127.42 (chlorophenyl C_1), 127.67 (chlorophenyl $\text{C}_{2,2'}$), 127.82 (methoxyphenyl $\text{C}_{2,2'}$), 129.08 (benzylidene $\text{C}_{2,2'}$), 131.22 (chlorophenyl $\text{C}_{3,3'}$), 132.41 (benzylidene C_1), 133.98 (chlorophenyl C_4), 136.22 (benzylidene $\text{C}_{3,3'}$), 140.12 (benzylidene C_4), 141.17 ($\text{C} = \text{N}$), 149.79 (thiazole C_4), 160.44 (methoxyphenyl C_4), 168.72 (thiazole C_2). HRMS (m/z): $[\text{M} + \text{H}]^+$ calcd for $\text{C}_{23}\text{H}_{18}\text{ClN}_3\text{OS}_2$: 452.0653; found: 451.0642.

3.4.12. 4-(4-Methoxyphenylsulfanyl)benzaldehyde [4-(4-fluorophenyl)-1,3-thiazol-2-yl] hydrazone (3l)

Yield: 92%, mp = 182.1 °C, FTIR (ATR, cm^{-1}): 3284 (N - H), 1489 ($\text{C} = \text{N}$), 1247 ($\text{C} - \text{N}$), 821, 732. ^1H NMR (300 MHz, DMSO- d_6): $\delta = 3.80$ (3H, s, OCH_3), 6.98–7.07 (2H, m, methoxyphenyl $\text{H}_{3,3'}$), 7.09–7.14 (2H, m, benzylidene $\text{H}_{2,2'}$), 7.20–7.30 (3H, m, fluorophenyl $\text{H}_{2,2'}$, thiazole H), 7.42–7.47 (2H, m, methoxyphenyl $\text{H}_{2,2'}$), 7.56 (2H, d, $J = 8.49$ Hz, benzylidene $\text{H}_{3,3'}$), 7.85–7.90 (2H, m, fluorophenyl $\text{H}_{3,3'}$), 7.94–7.96 (1H, m,

azomethine CH), 12.16 (1H, s, NH). ^{13}C NMR (75 MHz, DMSO- d_6): δ = 55.80 (OCH₃), 103.91 (thiazole C₅), 115.98 (methoxyphenyl C_{3,3'}), 122.65 (methoxyphenyl C₁), 127.41 (J_{CF-2} = 11.0 Hz, fluorophenyl C_{2,2'}), 127.83 (methoxyphenyl C_{2,2'}), 127.88 (benzylidene C_{2,2'}), 128.97 (fluorophenyl C₁), 130.26 (J_{CF-2} = 21.2 Hz, fluorophenyl C_{3,3'}), 132.44 (benzylidene C₁), 136.22 (benzylidene C_{3,3'}), 140.07 (benzylidene C₄), 141.07 (C = N), 149.86 (thiazole C₄), 160.44 (methoxyphenyl C₄), 162.04 (J_{CF-1} = 243.8 Hz, fluorophenyl C₄), 168.67 (thiazole C₂). HRMS (m / z): [M + H]⁺ calcd for C₂₃H₁₈FN₃OS₂: 436.0948; found: 436.0946.

3.4.13. 4-(4-Methoxyphenylsulfanyl)benzaldehyde [4-(2,4-dichlorophenyl)-1,3-thiazol-2-yl] hydrazone (3m)

Yield: 92%, mp = 103.7 °C, FTIR (ATR, cm⁻¹): 3168 (N - H), 1490 (C = N), 1249 (C - N), 1051, 821, 810. ^1H NMR (300 MHz, DMSO- d_6): δ = 3.80 (3H, s, OCH₃), 7.04 (2H, d, J = 8.85 Hz, methoxyphenyl H_{3,3'}), 7.13 (2H, d, J = 8.43 Hz, benzylidene H_{2,2'}), 7.39 (1H, s, thiazole H), 7.45 (2H, d, J = 8.85 Hz, methoxyphenyl H_{2,2'}), 7.49 (1H, dd, J = 2.22–8.49 Hz, dichlorophenyl H₅), 7.56 (2H, d, J = 8.52 Hz, benzylidene H_{3,3'}), 7.68 (1H, d, J = 2.16 Hz, dichlorophenyl H₃), 7.88 (1H, d, J = 8.49 Hz, dichlorophenyl H₆), 7.98 (1H, s, azomethine CH), 12.24 (1H, s, NH). ^{13}C NMR (75 MHz, DMSO- d_6): δ = 55.80 (OCH₃), 109.73 (thiazole C₅), 115.98 (methoxyphenyl C_{3,3'}), 122.48 (methoxyphenyl C₁), 127.46 (dichlorophenyl C₃), 127.82 (methoxyphenyl C_{2,2'}), 127.96 (benzylidene C_{2,2'}), 130.21 (dichlorophenyl C₅), 132.04 (dichlorophenyl C₁), 132.36 (dichlorophenyl C₆), 132.50 (benzylidene C₁), 132.68 (dichlorophenyl C₄), 132.99 (dichlorophenyl C₂), 136.22 (benzylidene C_{3,3'}), 140.19 (benzylidene C₄), 141.41 (C = N), 146.23 (thiazole C₄), 160.44 (methoxyphenyl C₄), 167.81 (thiazole C₂). HRMS (m / z): [M + H]⁺ calcd for C₂₃H₁₇Cl₂N₃OS₂: 486.0263; found: 486.0261.

3.4.14. 4-(4-Methoxyphenylsulfanyl)benzaldehyde [4-(2,4-difluorophenyl)-1,3-thiazol-2-yl] hydrazone (3n)

Yield: 88%, mp = 201.4 °C, FTIR (ATR, cm⁻¹): 3170 (N - H), 1489 (C = N), 1249 (C - N), 850, 821. ^1H NMR (300 MHz, DMSO- d_6): δ = 3.79 (3H, s, OCH₃), 6.99 (1H, m, difluorophenyl H₅), 7.03–7.09 (5H, m, methoxyphenyl H_{3,3'}, difluorophenyl H₃, benzylidene H_{2,2'}), 7.21 (1H, s, thiazole), 7.40–7.47 (2H, m, methoxyphenyl H_{2,2'}), 7.50–7.57 (2H, m, benzylidene H_{3,3'}), 7.56 (1H, d, J = 8.50 Hz, difluorophenyl H₆), 7.98 (1H, s, azomethine CH), 12.18 (1H, s, NH). ^{13}C NMR (75 MHz, DMSO- d_6): δ = 55.81 (OCH₃), 104.75 (t, J = 26.3 Hz, difluorophenyl C₃), 108.15 (d, J = 13.8 Hz, thiazole C₅), 112.34 (dd, J = 2.8–21.0 Hz, difluorophenyl C₅), 115.68 (methoxyphenyl C_{3,3'}), 119.52 (dd, J = 3.9–11.2 Hz, difluorophenyl C₁), 121.58 (methoxyphenyl C₁), 128.58 (methoxyphenyl C_{2,2'}), 129.26 (benzylidene C_{2,2'}), 130.83 (t, J = 10.2 Hz, difluorophenyl C₆), 137.70 (benzylidene C_{3,3'}), 141.62 (benzylidene C₄), 143.71 (C = N), 149.20 (thiazole C₄), 156.43, 159.66 (methoxyphenyl C₄), 160.02 (dd, J = 12.0–250.3 Hz, difluorophenyl C₄), 161.76 (dd, J = 12.6–245.7 Hz, difluorophenyl C₂), 166.75 (thiazole C₂). HRMS (m / z): [M + H]⁺ calcd for C₂₃H₁₇F₂N₃OS₂: 454.0854; found: 454.0849.

3.5. MAO-A and MAO-B inhibition assay

*h*MAO inhibitory activity of the compounds (3a–3n) was determined by a fluorometric method using the Bio-Vision MAO A/B (MAO-A/B) Inhibitor Screening Kit (USA) according to the manufacturer's instructions.^{19,20}

All pipetting processes were performed using a BioTek Precision XS robotic system (USA). Measurements were carried out with a BioTek Synergy H1 microplate reader (USA) based on the fluorescence generated (excitation, 535 nm; emission, 587 nm) over a 20-min period, in which the fluorescence increased linearly. Clorgiline and selegiline were used as the specific inhibitors of *h*MAO-A and *h*MAO-B, respectively.

Standard drugs and synthesized compounds were prepared at 10^{-3} to 10^{-9} M concentrations using 2% DMSO. Recombinant enzymes and developer were diluted in the reaction buffer. Substrate was diluted in bidistilled H₂O. In order to prepare the MAO working solution, 37 μ L of assay buffer, 1 μ L of developer solution, 1 μ L of substrate solution, and 1 μ L of OxiRed probe were mixed for each well.

The solutions of inhibitors and standard drugs (10 μ L/well) and recombinant enzyme solution (50 μ L/well) were added to a black flat-bottomed 96-well microplate and incubated for 10 min at 25 °C and 37 °C for the MAO-A and MAO-B assay, respectively. After this incubation period, the reaction was started by adding a working solution (40 μ L/well). The mixture was incubated for 30 min at a proper temperature. Fluorescence was measured using excitation at 535 nm and emission at 587 nm at 5-min intervals. Control experiments were carried out simultaneously by replacing the inhibitor solution with 2% DMSO (10 μ L). To check the probable inhibitory effect of the inhibitors on the developer, a parallel reading was performed by replacing enzyme solutions with 10 mM H₂O₂ solution (50 μ L/well). In addition, the possible capacity of the inhibitors to modify the fluorescence generated in the reaction mixture due to nonenzymatic inhibition was determined by mixing the inhibitor and working solutions.

The specific fluorescence values (used to obtain the final results) were calculated after subtraction of the background activity, which was determined from wells containing all components except for the *h*MAO isoforms, which were replaced by phosphate buffer (50 μ L/well). The blank, control, and all concentrations of inhibitors were analyzed in quadruplicate and inhibition percentage was calculated by using the following equation:

$$\% \text{Inhibition} = \frac{(\text{FC}_{t2} - \text{FC}_{t1}) - (\text{FI}_{t2} - \text{FI}_{t1})}{\text{FC}_{t2} - \text{FC}_{t1}} \times 100$$

FC_{t2} = Fluorescence of a control well measured at time t_2 ;

FC_{t1} = fluorescence of a control well measured at time t_1 ;

FI_{t2} = fluorescence of an inhibitor well measured at time t_2 ;

FI_{t1} = fluorescence of an inhibitor well measured at time t_1 .

The IC₅₀ values were calculated from a dose–response curve obtained by plotting the percentage inhibition versus the log concentration with the use of Microsoft Office Excel 2013. The results were displayed as mean \pm standard deviation. The SI was calculated as IC₅₀ (*h*MAO-A) / IC₅₀ (*h*MAO-B).

3.6. Enzyme kinetic studies

The same materials were used in the MAO inhibition assay. The most active compound against the *h*MAO-A enzyme, **3f**, was tested at five different concentrations (IC₅₀ / 4, IC₅₀ / 2, IC₅₀, 2 \times IC₅₀, and 4 \times IC₅₀). The inhibitor (10 μ L/well) and MAO-A enzyme solution (50 μ L/well) were added to the black flat-bottomed 96-well microplate and incubated at 37 °C for 10 min. After the incubation period, the working solution, including the reaction buffer, developer solution, OxiRed, and various concentrations (20, 10, 5, 2.5, 1.25, and 0.625 μ M) of tyramine (40 μ L/well), was added. The increase of the fluorescence (Ex/Em = 535 / 587 nm) was recorded for 30 min. A parallel experiment was carried out without inhibitor. All processes were assayed

in quadruplicate. The results were analyzed as Lineweaver–Burk plots²¹ using Microsoft Office Excel 2013. K_m and V_{max} values belonging to the inhibitor and control were calculated using junction points on the x- and y-axis. The slopes of the Lineweaver–Burk plots were replotted versus the inhibitor concentration and the inhibitory constant (K_i) was calculated.³²

3.7. Cytotoxicity assay

Cytotoxicity of compound **3f** was tested using the NIH/3T3 mouse embryonic fibroblast cell line (ATCC CRL1658, London, UK). NIH/3T3 cells were incubated according to the supplier's recommendations. NIH/3T3 cells were seeded at 1×10^4 cells into each well of 96-well plates. The MTT assay was performed as previously described.^{33,34} The compounds were tested between 0.0316 and 1000 μ M concentrations. The IC₅₀ values were determined by plotting a dose–response curve of inhibition % versus compound concentrations tested.³⁵

3.8. Prediction of ADME parameters and BBB permeability

Physicochemical parameters of the compounds (**3a–3n**) were analyzed by the online Molinspiration property calculation program (<http://www.molinspiration.com/services/properties.html>). BBB permeability of the compounds was assigned by the online BBB Predictor (<http://www.cbligand.org/BBB/index.php>).

References

1. Salgın-Gökşen, U.; Gökhan-Kelekçi, N.; Yabanoğlu-Çiftçi, S.; Yelekçi, K.; Uçar, G. *J. Neural. Transm. (Vienna)* **2013**, *120*, 883-891.
2. Patil, P. O.; Sanjay, B. B. *Arab. J. Chem.* **2014**, *7*, 857-884.
3. Tripathi, R. K.; Ayyannan, S. R. *ChemMedChem* **2016**, *11*, 1551-1567.
4. Garcia-Miralles, M.; Ooi, J.; Ferrari Bardile, C.; Tan, L. J.; George, M.; Drum, C. L.; Lin, R. Y.; Hayden, M. R.; Pouladi, M. A. *Exp. Neurol.* **2016**, *278*, 4-10.
5. D'Ascenzio, M.; Chimenti, P.; Gidaro, M. C.; De Monte, C.; De Vita, D.; Granese, A.; Scipione, L.; Di Santo, R.; Costa, G.; Alcaro, S. et al. *J. Enzyme Inhib. Med. Chem.* **2015**, *30*, 908-919.
6. Harris, S.; Johnson, S.; Duncan, J. W.; Udemgba, C.; Meyer, J. H.; Albert, P. R.; Lomberk, G.; Urrutia, R.; Ou, X. M.; Stockmeier, C. A. et al. *Neuropsychopharmacology* **2015**, *40*, 1373-1382.
7. Kaya, B.; Sağlık, B. N.; Levent, S.; Özkay, Y.; Kaplancıklı, Z. A. *J. Enzyme Inhib. Med. Chem.* **2016**, *31*, 1654-1661.
8. Chimenti, F.; Maccioni, E.; Secci, D.; Bolasco, A.; Chimenti, P.; Granese, A.; Carradori, S.; Alcaro, S.; Ortuso, F.; Yáñez, M. et al. *J. Med. Chem.* **2008**, *51*, 4874-4880.
9. Khattab, S. N.; Abdel Moneim, S. A.; Bekhit, A. A.; El Massry, A. M.; Hassan, S. Y.; El-Faham, A.; Ali Ahmed, H. E.; Amer, A. *Eur. J. Med. Chem.* **2015**, *93*, 308-320.
10. Kumar, B.; S, Sheetal.; Mantha, A. K.; Kumar, V. *RSC Adv.* **2016**, *6*, 42660-42683.
11. Finberg, J. P. *Pharmacol Ther.* **2014**, *143*, 133-152.
12. Badrey, M. G.; Gomha, S. M.; Arafa, W. A. A.; Abdulla, M. M. *J. Heterocyclic Chem.* **2017**, *54*, 1215-1227.
13. Chimenti, F.; Bolasco, A.; Secci, S.; Chimenti, P.; Granese, A.; Carradori, S.; Yáñez, M.; Orallo, F.; Ortuso, F.; Alcaro, S. *Bioorg. Med. Chem.* **2010**, *18*, 5715-5723.
14. Secci, D.; Bolasco, A.; Carradori, S.; D'Ascenzio, M.; Nescatelli, R.; Yáñez, M. *Eur. J. Med. Chem.* **2012**, *58*, 405-417.
15. Evranos-Aksöz, B.; Baysal, İ.; Yabanoğlu-Çiftçi, S.; Djikic, T.; Yelekçi, K.; Uçar, G.; Ertan, R. *Arch. Pharm.* **2015**, *348*, 743-756.

16. Tripathi, R. K.; Ayyannan, S. R. *ChemMedChem* **2016**, *11*, 1551-1567.
17. Carradori, S.; Rotili, D.; De Monte, C.; Lenoci, A.; D'Ascenzio, M.; Rodriguez, V.; Filetici, P.; Miceli, M.; Nebbioso, A.; Altucci, L. et al. *Eur. J. Med. Chem.* **2014**, *80*, 569-578.
18. Chimenti, F.; Maccioni, E.; Secci, D.; Bolasco, A.; Chimenti, P.; Granese, A.; Befani, O.; Turini, P.; Alcaro, S.; Ortuso, F. et al. *J. Med. Chem.* **2007**, *50*, 707-712.
19. BioVision. *Fluorometric Monoamine Oxidase A (MAO-A) Inhibitor Screening Kit*, Catalog No: K796-100, Data Sheet; BioVision: Milpitas, CA, USA, 2015.
20. BioVision. *Fluorometric Monoamine Oxidase B (MAO-B) Inhibitor Screening Kit*, Catalog No: K797-100, Data Sheet; BioVision: Milpitas, CA, USA, 2015.
21. Lineweaver, H.; Burk, D. *J. Am. Chem. Soc.* **1934**, *57*, 658-666.
22. Pozzolini, M.; Scarfi, M. S.; Benatti, U.; Giovine, M. *Anal. Biochem.* **2003**, *313*, 338-341.
23. Mosmann, T. *J. Immunol. Methods* **1983**, *65*, 55-63.
24. International Organization for Standardization. *Biological Evaluation of Medical Devices-Part 5: Tests for In Vitro Cytotoxicity ISO-10993-5, 3rd ed.*; International Organization for Standardization: Geneva, Switzerland, 2009.
25. van de Waterbeemd, H.; Gifford, E. *Nat. Rev. Drug Discov.* **2003**, *2*, 192-204.
26. Lipinski, C. A.; Lombardo, F.; Dominy, B. W.; Feeney, P. J. *Adv. Drug Deliv. Rev.* **2001**, *46*, 3-26.
27. Ertl, P.; Rohde, B.; Selzer, P. *J. Med. Chem.* **2000**, *43*, 3714-3717.
28. Carpenter, T. S.; Kirshner, D. A.; Lau, E.Y.; Wong, S. E.; Nilmeier, J. P.; Lightstone, F. C. *Biophysical J.* **2014**, *107*, 630-641.
29. Lysek, R. *Helv. Chim. Acta* **2005**, *88*, 2788-2811.
30. Jampilek, J. *Chem. Pap.* **2005**, *59*, 182-186.
31. Bayer, GB Patent No: 694602, 1953.
32. Bradford, M. M. *Anal. Biochem.* **1976**, *72*, 248-254.
33. Demir Özkay, Ü.; Can, Ö. D.; Sağlık, B. N.; Acar Çevik, U.; Levent, S.; Özkay, Y.; Ilgin, S.; Atlı, Ö. *Bioorg. Med. Chem. Lett.* **2016**, *26*, 5387-5394.
34. Sağlık, B. N.; Ilgin, S.; Özkay, Y. *Eur. J. Med. Chem.* **2016**, *124*, 1026-1040.
35. Patel, S.; Gheewala, N.; Suthar, A.; Shah, A. *Int. J. Pharm. Sci.* **2009**, *1*, 38-46.